Turk J Elec Eng & Comp Sci, Vol.20, No.Sup.1, 2012, © TÜBİTAK
doi:10.3906/elk-1101-1059

PI and PID stabilization of neutral and retarded systems with time delay

Serdar Ethem HAMAMCI
Department of Electrical-Electronics Engineering, Faculty of Engineering,
İnönü University, 44280 Malatya-TURKEY
e-mail: serdar.hamamci@inonu.edu.tr

Received: 27.01.2011

Abstract

Stabilization using fixed-order controllers is one of the key topics in control system design for the linear time-invariant (LTI) systems. In this paper, the stabilization of LTI neutral and retarded time-delay systems by means of PI and PID controllers is investigated in detail. The basic theme of the presented approach is to obtain a global stability region in the 2-dimensional (2-D) (k_p, k_i)-plane for the PI controller and in the 3-dimensional (3-D) (k_p, k_i, k_d)-space for the PID controllers. This region is formed by stability boundaries that are defined as the real root boundary, infinite root boundary, and complex root boundary. The 3-D global stability region for the PID case is made up of the set of 2-D stability regions that are obtained in the (k_p, k_i)-plane, (k_p, k_d)-plane, or (k_i, k_d)-plane by changing the other third parameter. To achieve this, the stability boundary locus approach is incorporated into the D-decomposition method. Thus, the complete set of stabilizing PI and PID controllers for the system is obtained. The simulation results indicate that the presented stabilization method is effective and practically useful in the analysis and control of the neutral and retarded time-delay systems.

Key Words: *Neutral and retarded systems, state delay, stabilization, PI controllers, PID controllers*

1. Introduction

Delay differential equations are often preferred for the modeling of real plants, including the delay effect to the classical system description given by the ordinary differential equations [1]. Systems represented by a set of delay differential equations are called time-delay systems. In general, the time-delay systems can be grouped into 2 classes. One uses the system model with time delay in the control input. The other utilizes the system model with time delay in the state [2]. Studies on stability analysis and control of the first type of systems have been widely investigated in the last 3 decades [3,4]. However, the second class of time-delay systems, which is categorized into neutral systems and retarded systems, has been less studied than the first type in the literature [5]. Many time-delay systems that can be modeled by neutral and retarded differential equations are used in various disciplines, including lumped parameter networks interconnected by transmission lines, turbojet engine systems, the industrial systems containing steam lines, and some chemical reactors [6-8]. In recent years, some

studies related to the control of neutral and retarded time-delay systems that are based on modern control techniques such as the pole-placement method [9], linear-quadratic regulator control [10], and sliding mode control [11] have been reported in the literature. However, the control of neutral and retarded systems using simple and fixed-order controllers like first-order, proportional-integral (PI), and proportional-integral-derivative (PID) controllers is not prevalent.

It is surely beyond doubt that the PI and PID controllers are the most ubiquitous controllers used by control system designers due to the simplicity of their structures and facility in their implementations [4]. Theoretical research on these controllers was initiated in the mid-1900s after the works of Ziegler and Nichols [12]. Since then, an extensive amount of studies have been conducted in the fields of tuning methods, identification rules, and stabilization techniques [2,4,13]. In the stabilization area, the main purpose is to determine all of the stabilizing PI or PID controller values for the plant, as in the Youla parameterization [14]. Many stabilization algorithms using these controllers for the linear time-invariant (LTI) time-delay systems have been presented in the literature. For instance, Datta et al. [15] proposed a method using the extension of the Hermite-Biehler theorem applicable to quasipolynomials. Bajcinca [16] used the parameter space approach [17] based on the singular frequencies concept. The stability boundary locus method, which obtains a stability region using graphical relations in the parameter space, was presented by Tan [18]. The fractional-order PID stabilization of the integer and fractional-order systems with time delay was reported in [19] and [20] using Neimark's D-decomposition method [21]. However, the PI and PID stabilization processes taken into account in all of these cases deal entirely with systems with a single time delay in the control input or measurement output. For the neutral and retarded time-delay systems, stabilization using PI and PID controllers is an open problem, since these systems include a state delay and therefore have complicated system structures whose dynamics are also affected by past states. To the best of the author's knowledge, only 2 PI and PID stabilization studies in relation to H_∞ stability are available in the literature [22,23], but no studies are found concerning asymptotic stability. The formulation and simulations presented for neutral and retarded systems in this paper are intended to fill this gap.

In this paper, a practical algorithm for the solution to the question of determining all PI controllers that stabilize a neutral or a retarded system is introduced. This algorithm presents a method that determines the global stability region in the $(k_p,\ k_i)$-plane using stability boundaries so that all of the controller parameters within this region stabilize the given plant. For stability boundaries, analytical and straightforward expressions are derived using the results of the D-decomposition method [21]. Furthermore, an enhancement of the presented approach to the case of PID stabilization is also provided. The global stability region enclosing all of the stabilizing values of the PID parameters for a given plant is obtained in the $(k_p,\ k_i,\ k_d)$-space. There are 3 ways to determine the 3-dimensional (3-D) stability region: 1) a set of 2-dimensional (2-D) stability regions obtained by changing k_d in the $(k_p,\ k_i)$ plane, 2) a set of 2-D stability regions obtained by changing k_i in the $(k_p,\ k_d)$ plane, and 3) a set of 2-D stability regions obtained by changing k_p in the $(k_i,\ k_d)$ plane. The first 2 ways are possible in the D-decomposition method while the last is impossible, as will be clarified in Section 5. Therefore, the stability boundary locus method [18] and the D-decomposition method were combined for this case. Hence, a set of convex stability regions were obtained by changing k_p in the $(k_i,\ k_d)$ plane graphically. The advantage of this approach is that investigating the stability range of proportional gain with complex calculations as in the Hermite-Biehler method is not required, nor is it necessary to compute the singular frequencies for the proportional gain, as in the parameter space approach. The algorithm offered in this study

is important because it can be applied to the stabilization of neutral and retarded systems with parametric uncertainties.

2. Fundamentals of neutral and retarded time-delay systems

Time-delay systems with state delay belong to the class of infinite dimensional systems [1]. Following the classification given by Cooke [24] for these systems, we may have the systems of neutral type, advanced argument type, or delayed argument type (also known as the retarded case) [3]. Since the advanced argument case has no practical significance (no causality), the present study focuses only on the neutral and retarded cases.

Definition 2.1. *A LTI neutral time-delay system (NTDS) is defined by state-space equations with a delayed state vector and the derivative of the delayed state vector. Consider the state-space representation of the single-input, single-output NTDS given as the following expression:*

$$\dot{x}(t) = Ax(t) + A_1x(t-\tau) + A_2\dot{x}(t-\tau) + Bu(t)$$

$$y(t) = Cx(t), \tag{1}$$

where $x(t) \in \mathrm{R}^n$ *denotes the state vector while* $u(t) \in \mathrm{R}$ *and* $y(t) \in \mathrm{R}$ *are the control input and output variables, respectively. In addition,* A, A_1, $A_2 \in \mathrm{R}^{nxn}$, $B \in \mathrm{R}^{nx1}$, *and* $C \in \mathrm{R}^{1xn}$ *are the known constant matrices, and* $\tau \in \mathrm{R}^+$ *is the state delay.*

The transfer function of the NTDS given in Eq. (1) can be obtained as:

$$G(s) = \frac{Y(s)}{U(s)} = C(sI - A - A_1e^{-\tau s} - A_2se^{-\tau s})^{-1}B. \tag{2}$$

Definition 2.2. *A LTI retarded time-delay system (RTDS) is described by the state-space representation including only the term of the delayed state vector. The state-space equations of the RTDS have the general form:*

$$\dot{x}(t) = Ax(t) + A_1x(t-\tau) + Bu(t),$$

$$y(t) = Cx(t). \tag{3}$$

Note that the RTDS is a simple subclass of the NTDS for $A_2 = 0$ *in Eq. (1). The transfer function of the RTDS is given in the form:*

$$G(s) = \frac{Y(s)}{U(s)} = C(sI - A - A_1e^{-\tau s})^{-1}B. \tag{4}$$

By making the matrix operations in Eq. (2), the transfer function of the NTDS can be transformed to a rational transfer function form as:

$$G(s) = \frac{N(s)}{D(s)} = \frac{\sum\limits_{i=0}^{n-1}\sum\limits_{k=0}^{n-1} b_{ik}s^ie^{-k\tau s}}{\sum\limits_{i=0}^{n}\sum\limits_{k=0}^{n} a_{ik}s^ie^{-k\tau s}}, \tag{5}$$

where a_{ik} and b_{ik} are the arbitrary real constants. In Eq. (5), $N(s)$ and $D(s)$ are the quasipolynomials, which have no common factors in $\{Re\ s \geq 0\} \setminus \{0\}$. If some coefficients in Eq. (5) are 0, as follows:

$$\begin{array}{lll} b_{i(n-1+k-i)} = 0; & \text{for} \quad i = 1 \sim (n-1) & \text{and} \quad k = 1 \sim i \\ a_{i(n+k-i)} = 0; & \text{for} \quad i = 1 \sim n & \text{and} \quad k = 1 \sim i \end{array} \tag{6}$$

a rational transfer function for the RTDS is obtained. It follows from Eqs. (5) and (6) that the analysis and control of the neutral systems are more difficult than those of the retarded systems.

There are important differences between the pole distributions of the neutral and retarded time-delay systems. For the retarded system, the number of poles that are arranged to the right of the vertical stripe drawn in any real α is always limited, as seen in [25]. The poles of the RTDS are usually located as a finite number of pole sequences asymptotically departing to the upper-left direction from the origin. For the neutral systems, the poles of the system are arranged within the stripes drawn in some specific real α and β. The poles of the NTDS are also located as a finite number of asymptotic sequences. In spite of these differences in their pole distributions, the stability for the NTDS and RTDS is equivalent to the condition that all of the poles of the transfer function in Eq. (5) lie in the open left half plane (LHP) of the complex plane [2]. Interested readers may refer to [1] for details of the pole distributions and the stability issues of the NTDS and RTDS.

3. D-decomposition method from the viewpoint of control theory

Consider a characteristic polynomial of a closed-loop system including n real-valued unknown controller parameters:

$$P(s; x_1, x_2, ...x_n) = P_0(s) + \sum_{i=1}^{n} P_i(s)x_i = P_0(s) + P_1(s)x_1 + ... + P_{n-1}(s)x_{n-1} + P_n(s)x_n, \tag{7}$$

where $P_0(s)$ and $P_i(s)$ are simple polynomials. The aim is to find the unknown controller parameters x_1, x_2,..., x_n, which make the closed loop system asymptotically stable. There is such a stability domain $\boldsymbol{S}$ in the parameter space that for any point (x_1, x_2,..., x_n) $\in \boldsymbol{S}$, the characteristic equation $P(s; x_1, x_2, ...x_n)$ has only LHP roots. The other domains have the instability property such that at least one root is in the right half plane (RHP). Hence, finding the stability domain is a significant job for the controller design. This method is called the D-decomposition method, which was proposed by Neimark [21]. The D-decomposition method is a powerful graphical technique for stability analysis and design of control systems [19,26].

Accordingly, as a root passes the imaginary axis at the origin, infinity, or any location, 3 different types of stability boundaries isolating the stability region from the instability regions can be described as follows [17,19]:

- Real root boundary (RRB): If any real root passes through the origin, this boundary occurs. The equation of the RRB is determined by $P(s; x_1, x_2, ...x_n)|_{s=0} = 0$.

- Infinite root boundary (IRB): If any real root passes the vertical axis of the s-plane at s = ∞, this boundary is formed. The equation of IRB is found by $P(s; x_1, x_2, ...x_n)|_{s=\infty} = 0$ for Eq. (7). In this case, the characteristic polynomial has a degree drop; that is, the largest coefficient of the polynomial is equal to 0.

- Complex root boundary (CRB): This boundary takes place in the parameter space when any pair of complex roots passes the vertical axis of the s-plane at s = jω . In this case, the real and imaginary parts of Eq. (7) are equal to 0, i.e. $P(s; x_1, x_2, ...x_n)|_{s=\mp j\omega} = 0$.

Using these boundaries, the imaginary axis in the complex plane is mapped into parameter space $\boldsymbol{P}$. This mapping decomposes the parameter space into root invariant areas. All of the points $(x_1, x_2, \ldots, x_n)$ in a root invariant area result in a fixed number of stable and unstable control system poles. If an area does not include any RHP poles, then stabilizing controllers exist for the plant being considered. If no such area exists, then it is not possible to stabilize the given plant [27,28]. This is the basic idea of the D-decomposition approach.

4. Stabilization using a PI controller

Consider the block diagram of the stabilization problem shown in Figure 1. Here, $G(s)$ is the plant given in Eq. (5) and $C(s)$ is a PI controller denoted by:

$$C(s) = k_p + \frac{k_i}{s} = \frac{k_p s + k_i}{s}. \tag{8}$$

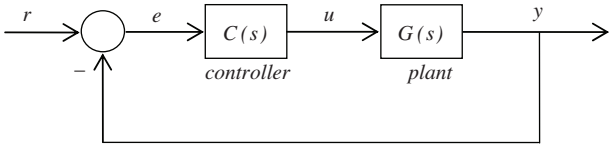

Figure 1. Block diagram of the stabilization problem.

Let y denote the output of the control system in Figure 1 defined as:

$$y = \frac{G(s)C(s)}{1 + G(s)C(s)} r, \tag{9}$$

where r is the reference input.

Definition 4.1. *The denominator of Eq. (9) is always a quasipolynomial since it includes terms with time delay. Therefore, the characteristic equation of the closed-loop system is defined as the transcendental characteristic equation (TCE). A general form of the TCE for the NTDS and RTDS is represented by:*

$$P(s) = 1 + G(s)C(s) = \sum_{i=0}^{n} \sum_{k=0}^{n} p_{ik} s^i e^{-k\tau s} \tag{10}$$

$$= (p_{00} + p_{10}s + \ldots + p_{n0}s^n) + (p_{01} + p_{11}s + \ldots + p_{n1}s^n)e^{-\tau s} + \ldots + (p_{0n} + p_{1n}s + \ldots + p_{nn}s^n)e^{-n\tau s},$$

where p_{ik} are the real coefficients.

Putting Eqs. (5) and (8) into Eq. (10), the TCE of the closed-loop system becomes:

$$P(s; k_p, k_i) = sD(s) + (k_p s + k_i)N(s) = \sum_{i=0}^{n} \sum_{k=0}^{n} a_{ik} s^{i+1} e^{-k\tau s} + \sum_{i=0}^{n-1} \sum_{k=0}^{n-1} \left[b_{ik} \left(k_p s^{i+1} + k_i s^i \right) e^{-k\tau s} \right]. \tag{11}$$

For the PI controller parameters k_p and k_i, the closed-loop system is said to be asymptotically stable if the characteristic equation $P(s; k_p, k_i)$ has no roots in the RHP of the complex plane.

By applying the descriptions in Section 3 to the TCE in Eq. (11), the RRB is determined as a line:

$$k_i = 0. \tag{12}$$

Because the order of the denominator is larger than that of the numerator in the $G(s)C(s)$ transfer function, the IRB for the PI case does not exist. This can also be seen by equating the coefficient of the largest order of the TCE in Eq. (11) to 0.

For the construction of the CRB, we substitute $s = j\omega$ into Eq. (11) and equate it to 0 to obtain:

$$P(\omega; k_p, k_i) = \sum_{i=0}^{n}\sum_{k=0}^{n} a_{ik}(j\omega)^{i+1}e^{-j\omega k\tau} + \sum_{i=0}^{n-1}\sum_{k=0}^{n-1}\left[b_{ik}\left(k_p(j\omega)^{i+1} + k_i b_{ik}(j\omega)^i\right)e^{-j\omega k\tau}\right] = 0, \tag{13}$$

which is equivalent to:

$$\sum_{i=0}^{n}\sum_{k=0}^{n} a_{ik}j^{i+1}\omega^{i+1}(\cos k\tau\omega - jsink\tau\omega) + \sum_{i=0}^{n-1}\sum_{k=0}^{n-1}\left[b_{ik}\left(k_p j^{i+1}\omega^{i+1} + k_i b_{ik}j^i\omega^i\right)(\cos k\tau\omega - jsink\tau\omega)\right] = 0. \tag{14}$$

The terms j^i and j^{i+1} can be stated by the following ordinary complex numbers:

$$j^i = \cos i\frac{\pi}{2} + j\sin i\frac{\pi}{2} = x_i + jy_i, \tag{15}$$

$$j^{i+1} = \cos(i+1)\frac{\pi}{2} + j\sin(i+1)\frac{\pi}{2} = z_i + jt_i. \tag{16}$$

Hence, $P(\omega; k_p, k_i)$ in Eq. (13) can be written as:

$$\begin{aligned}
&\sum_{i=0}^{n}\sum_{k=0}^{n} a_{ik}(z_i + jt_i)\omega^{i+1}(\cos k\tau\omega - jsink\tau\omega)\\
&+\sum_{i=0}^{n-1}\sum_{k=0}^{n-1}\left[b_{ik}\left(k_p(z_i + jt_i)\omega^{i+1} + k_i(x_i + jy_i)\omega^i\right)(\cos k\tau\omega - jsink\tau\omega)\right]\\
&= \Re\{P(\omega; k_p, k_i)\} + j\Im\{P(\omega; k_p, k_i)\} = 0,
\end{aligned} \tag{17}$$

where $\Re\{P(\omega; k_p, k_i)\}$ and $\Im\{P(\omega; k_p, k_i)\}$ are the real and imaginary parts of Eq. (17), respectively. By equating the real and imaginary parts to 0, we obtain the following 2-D equation set:

$$\begin{aligned}
k_p A(\omega) + k_i C(\omega) &= E(\omega)\\
k_p B(\omega) + k_i D(\omega) &= F(\omega)
\end{aligned}, \tag{18}$$

where

$$A(\omega) = \sum_{i=0}^{n-1}\sum_{k=0}^{n-1} b_{ik}\omega^{i+1}(z_i\cos k\tau\omega + t_i\sin k\tau\omega), \tag{19a}$$

$$B(\omega) = \sum_{i=0}^{n-1}\sum_{k=0}^{n-1} b_{ik}\omega^{i+1}(-z_i\sin k\tau\omega + t_i\cos k\tau\omega), \tag{19b}$$

$$C(\omega) = \sum_{i=0}^{n-1}\sum_{k=0}^{n-1} b_{ik}\omega^{i}(x_i\cos k\tau\omega + y_i\sin k\tau\omega), \tag{19c}$$

$$D(\omega) = \sum_{i=0}^{n-1}\sum_{k=0}^{n-1} b_{ik}\omega^i\,(-x_i \sin k\tau\omega + y_i \cos k\tau\omega), \tag{19d}$$

$$E(\omega) = -\sum_{i=0}^{n}\sum_{k=0}^{n} a_{ik}\omega^{i+1}\,(z_i \cos k\tau\omega + t_i \sin k\tau\omega), \tag{19e}$$

$$F(\omega) = -\sum_{i=0}^{n}\sum_{k=0}^{n} a_{ik}\omega^{i+1}\,(-z_i \sin k\tau\omega + t_i \cos k\tau\omega). \tag{19f}$$

The solution for Eq. (18) is given by:

$$k_p = [D(\omega)E(\omega) - C(\omega)F(\omega)]/\Delta(\omega), \tag{20}$$

$$k_i = [A(\omega)F(\omega) - B(\omega)E(\omega)]/\Delta(\omega), \tag{21}$$

where $\Delta(\omega) = A(\omega)D(\omega) - B(\omega)C(\omega)$. Changing ω from 0 to ∞ in Eqs. (20) and (21), the CRB is constructed as a curve in the $(k_p,\ k_i)$-plane.

Corollary 4.1. *The parameter plane $(k_p,\ k_i)$ is partitioned into stable and unstable areas by the RRB and CRB. The stable areas can be attained by testing any check point in each area. The TCE associated with the stable area has roots only with negative real parts. In order to test a TCE's stability, some effective and useful algorithms reported in [6] and [29] can be used. The area that has the stable TCE is defined as the global stability region, which includes a set of all stabilizing PI parameters.*

To clarify the PI stabilization process presented in this section, the example below is examined.

4.1. Example

Consider the LTI neutral system with the following system matrices:

$$A = \begin{bmatrix} -0.9 & 0.2 \\ 0.1 & -0.9 \end{bmatrix}, \quad A_1 = \begin{bmatrix} -1.1 & -0.2 \\ -0.1 & -1.1 \end{bmatrix}, \quad A_2 = \begin{bmatrix} -0.2 & 0 \\ 0.2 & -0.1 \end{bmatrix}, \tag{22}$$

which was examined for stability analysis in [29] and was reported as a system that is asymptotically stable for $\tau \leq 2.225$. For the control vector $B = \begin{bmatrix} 1 & 1 \end{bmatrix}^T$ and the output vector $C = \begin{bmatrix} 1 & 0 \end{bmatrix}$, the transfer function of the system is obtained as:

$$G(s) = \frac{(s+1.1) + (0.1s+0.9)e^{-\tau s}}{(s^2+1.8s+0.79) + (0.3s^2+2.43s+2.02)e^{-\tau s} + (0.02s^2+0.37s+1.19)e^{-2\tau s}}. \tag{23}$$

In this example, the unstable system case is selected. Therefore, the value of the time delay is taken into account as $\tau = 3$. The purpose is to get all of the stabilizing PI controllers for the system given in Eq. (23).

In consideration of Eqs. (20) and (21), the CRB equations are determined by:

$$k_p = \frac{\begin{pmatrix} 0.673\omega^2 + 2.687 + (1.399\omega^2 + 4.004)\cos(3\omega) + (0.202\omega^2 - 0.674)\omega\sin(3\omega) \\ +(0.348\omega^2 + 1.309)\cos(6\omega) + (0.02\omega^2 - 0.783)\omega\sin(6\omega) \end{pmatrix}}{-1.01\omega^2 - 2.02 - (0.2\omega^2 + 1.98)\cos(3\omega) + 1.58\omega\sin(3\omega)}, \tag{24}$$

$$k_i = \frac{\left(\begin{array}{l} -1.03\omega^4 - 3.175\omega^2 - (0.402\omega^2 + 2.408)\omega^2 \cos(3\omega) + (2.839\omega^2 + 2.582)\omega \sin(3\omega) \\ +(-0.02\omega^2 + 0.783)\omega^2 \cos(6\omega) + (0.348\omega^2 + 1.309)\omega \sin(6\omega) \end{array} \right)}{-1.01\omega^2 - 2.02 - (0.2\omega^2 + 1.99)\cos(3\omega) + 1.58\omega \sin(3\omega)}. \quad (25)$$

The RRB line defined in Eq. (12) and the CRB curve obtained depending on ω in Eqs. (24) and (25) are shown in Figure 2a, where it can be seen that the boundaries decompose the complete parameter plane into many areas. By taking any check point in any area and applying the stability method presented in [29], the global stability region, which is illustrated by the colored area in Figure 2, is obtained. The PI controllers corresponding to the (k_p, k_i) points in the colored area cause the poles of the closed loop system to be located completely in the LHP. Figure 2b shows the boundary values of k_i when k_p is chosen as 0.5. From this, the TCE is stable for $k_i \in (0, 1.08) \cup (1.834, 8.107)$. On a large scale, the CRB curve has a growing helix form proportional with ω, as shown in Figure 3. In this case, the curve is plotted for a wide range of ω, from 0 to 29.07.

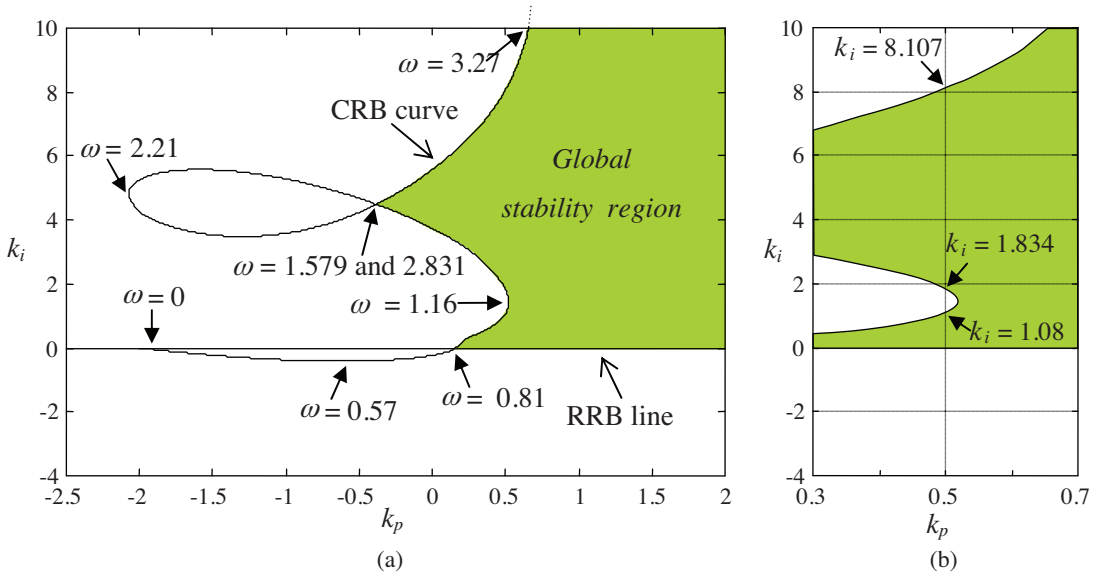

Figure 2. a) The global stability region for $\omega \in [0, 3.27]$ and b) the boundary values of k_i for $k_p = 0.5$.

Finally, to verify the results, the pole distributions of the PI control system choosing some points in the (k_p, k_i)-plane can be examined. Pole spectrums of the control system for $k_i = 4.5$, 8.107 and 10, when taking $k_p = 0.5$ as fixed, are shown in Figure 4. Furthermore, for the same purpose and the controller parameter values, the unit step responses of the PI control system can be plotted, as shown in Figure 5. As can be seen from Figures 4 and 5, the PI control system is asymptotically stable for the controller parameters (k_p, k_i) = (0.5, 4.5) in the global stability region, marginally stable for the controller parameters (k_p, k_i) = (0.5, 8.107) on the CRB boundary curve, and unstable for the controller parameters (k_p, k_i) = (0.5, 10) outside of the global stability region. The results indicated by the Figures in this example conclude that the presented stabilization technique is a successful and easy approach to obtain the stabilizing PI controllers for the neutral (and retarded) systems.

5. Stabilization using PID controller

In this section, the steps of PI stabilization for the neutral and retarded time-delay systems are extended to the PID case. The TCE of the closed-loop system for this case is in the following form:

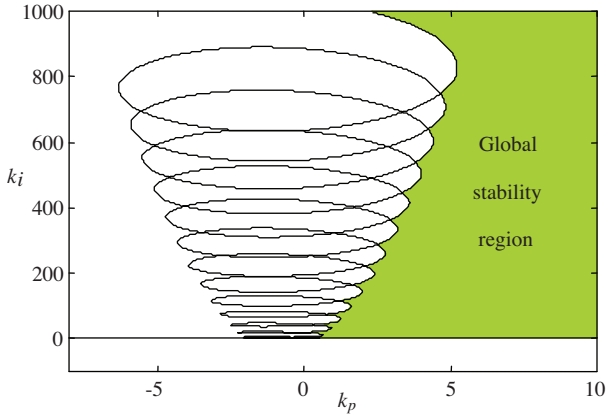

Figure 3. The large scale global stability region for $\omega \in [0, 29.07]$.

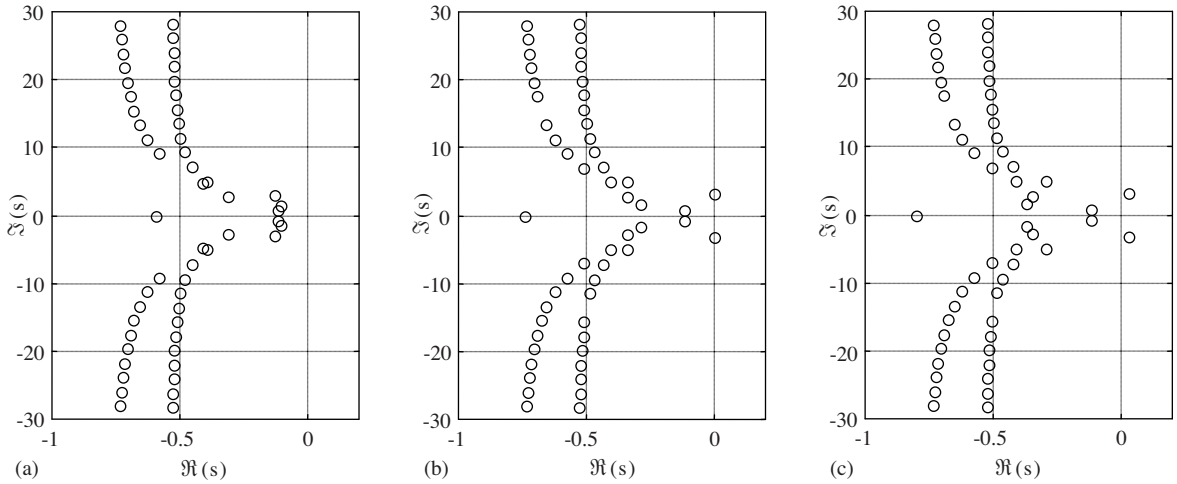

Figure 4. The pole distributions of the PI control system: a) $k_p = 0.5$ and $k_i = 4.5$ (asymptotically stable case), b) $k_p = 0.5$ and $k_i = 8.107$ (marginally stable case), and c) $k_p = 0.5$ and $k_i = 10$ (unstable case).

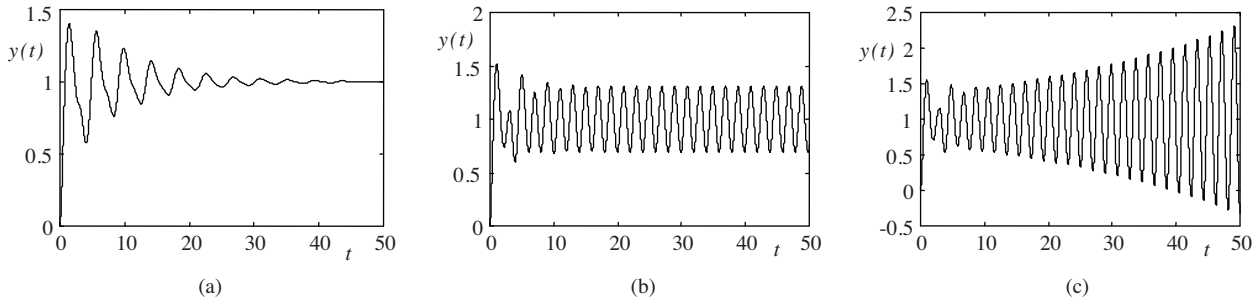

Figure 5. The unit step responses of the PI control system: a) $k_p = 0.5$ and $k_i = 4.5$ (asymptotically stable case), b) $k_p = 0.5$ and $k_i = 8.107$ (marginally stable case), and c) $k_p = 0.5$ and $k_i = 10$ (unstable case).

$$P(s;k_p,k_i,k_d)=\sum_{i=0}^{n}\sum_{k=0}^{n}a_{ik}s^{i+1}e^{-k\tau s}+\sum_{i=0}^{n-1}\sum_{k=0}^{n-1}\left[b_{ik}\left(k_ds^{i+2}+k_ps^{i+1}+k_is^{i}\right)e^{-k\tau s}\right]. \tag{26}$$

Considering $P(s;x_1,x_2,...x_n)|_{s=0}=0$ in Eq. (26), the PID stabilization has the same RRB as in the PI case. However, because the order of the numerator is equal to that of the denominator for the $G(s)C(s)$ transfer function, there exists an IRB such that:

$$a_{nn}+b_{(n-1)(n-1)}k_d=0, \tag{27}$$

found by $P(s;x_1,x_2,...x_n)|_{s=\infty}=0$ for the PID controller.

For the CRB, the 2-D equation system is now obtained with 3 unknowns as follows:

$$\begin{array}{l} k_pA(\omega)+k_iC(\omega)+k_dG(\omega)=E(\omega) \\ k_pB(\omega)+k_iD(\omega)+k_dH(\omega)=F(\omega) \end{array}, \tag{28}$$

where

$$G(\omega)=\sum_{i=0}^{n-1}\sum_{k=0}^{n-1}b_{ik}\omega^{i+2}\left(q_i\cos k\tau\omega+r_isink\tau\omega\right), \tag{29a}$$

$$H(\omega)=\sum_{i=0}^{n-1}\sum_{k=0}^{n-1}b_{ik}\omega^{i+2}\left(-q_i\sin k\tau\omega+r_icosk\tau\omega\right), \tag{29b}$$

where

$$q_i=\Re\left\{j^{i+2}\right\}=\cos(i+2)\frac{\pi}{2}\text{ and }r_i=\Im\left\{j^{i+2}\right\}=\sin(i+2)\frac{\pi}{2}. \tag{30}$$

Since the number of unknowns is greater than the number of equations, the solution for the CRB can only be obtained depending upon one of the controller parameters. It follows from Eq. (28) that the CRB curve can be expressed in the $(k_p,\ k_i)$-plane in terms of k_d, in the $(k_p,\ k_d)$-plane in terms of k_i, or in the $(k_i,\ k_d)$-plane in terms of k_p.

The controller parameters k_p and k_i to construct the CRB in the $(k_p,\ k_i)$-plane in terms of k_d are determined from the solution of Eq. (28).

$$k_p=\left[\left(C(\omega)H(\omega)-D(\omega)G(\omega)\right)k_d+\left(D(\omega)E(\omega)-C(\omega)F(\omega)\right)\right]/\Delta_1(\omega), \tag{31}$$

$$k_i=\left[\left(B(\omega)G(\omega)-A(\omega)H(\omega)\right)k_d+\left(A(\omega)F(\omega)-B(\omega)E(\omega)\right)\right]/\Delta_1(\omega), \tag{32}$$

where $\Delta_1(\omega)=A(\omega)D(\omega)-B(\omega)C(\omega)$. Similarly, to obtain the CRB in the $(k_p,\ k_d)$-plane in terms of k_i, the controller parameters k_p and k_d are calculated as follows:

$$k_p=\left[\left(C(\omega)H(\omega)-D(\omega)G(\omega)\right)k_i+\left(F(\omega)G(\omega)-E(\omega)H(\omega)\right)\right]/\Delta_2(\omega), \tag{33}$$

$$k_d=\left[\left(A(\omega)D(\omega)-B(\omega)C(\omega)\right)k_i+\left(B(\omega)E(\omega)-A(\omega)F(\omega)\right)\right]/\Delta_2(\omega), \tag{34}$$

where $\Delta_2(\omega)=B(\omega)G(\omega)-A(\omega)H(\omega)$. Finally, to determine the CRB in the $(k_i,\ k_d)$-plane in terms of k_p, the controller parameters k_i and k_d are obtained by:

$$k_i=\left[\left(B(\omega)G(\omega)-A(\omega)H(\omega)\right)k_p+\left(E(\omega)H(\omega)-F(\omega)G(\omega)\right)\right]/\Delta_3(\omega), \tag{35}$$

$$k_d = [(A(\omega)D(\omega) - B(\omega)C(\omega))\,k_p + (C(\omega)F(\omega) - D(\omega)E(\omega))]/\Delta_3(\omega), \tag{36}$$

where $\Delta_3(\omega) = C(\omega)H(\omega) - D(\omega)G(\omega)$.

Corollary 5.1. *It is impossible to find a solution for the CRB in the $(k_i\,,\ k_d)$-plane in terms of k_p, since the denominator of Eqs. (35) and (36), i.e. $\Delta_3(\omega)$, is always equal to 0. However, it should be noted that $\Delta_3(\omega)$ being 0 does not necessarily mean that there is no $(k_i\,,\ k_d)$ pair whose closed-loop poles cross over the imaginary axis for a given k_p value. On the contrary, as will be shown in Remark 5.2, there must be such values in the $(k_i\,,\ k_d)$-plane, since there exist solutions for the other 2 planes.*

Proof. Substituting Eqs. (19c), (19d), (29a), and (29b) for $\Delta_3(\omega)$, we obtain:

$$\begin{aligned}\Delta_3(\omega) \;=\; & \left[\sum_{i=0}^{n-1}\sum_{k=0}^{n-1} b_{ik}\omega^i\,(x_i\cos k\tau\omega + y_i\sin k\tau\omega)\right]\left[\sum_{i=0}^{n-1}\sum_{k=0}^{n-1} b_{ik}\omega^{i+2}\,(-q_i\sin k\tau\omega + r_i\cos k\tau\omega)\right] \\ & - \left[\sum_{i=0}^{n-1}\sum_{k=0}^{n-1} b_{ik}\omega^i\,(-x_i\sin k\tau\omega + y_i\cos k\tau\omega)\right]\left[\sum_{i=0}^{n-1}\sum_{k=0}^{n-1} b_{ik}\omega^{i+2}\,(q_i\cos k\tau\omega + r_i\sin k\tau\omega)\right]\end{aligned}. \tag{37}$$

Let the time-delay system be a first-order one. Hence, Eq. (37) simply becomes:

$$\Delta_3(\omega) = (b_{00}x_0)(b_{00}\omega^2 r_0) - (b_{00}y_0)(b_{00}\omega^2 q_0). \tag{38}$$

Putting the values $x_0 = 1$, $y_0 = 0$, $q_0 = -1$, and $r_0 = 0$, which are obtained from Eqs. (15) and (30), into the above equation, the determinant is readily obtained as $\Delta_3(\omega) = 0$.

For $n \geq 2$, the proof follows from applying the above procedure to Eq. (37). □

Remark 5.1. *Since $\Delta_1(\omega)$ and $\Delta_2(\omega)$ are different from 0, the CRB is found directly in the $(k_p\,,\ k_i)$-plane using Eqs. (31) and (32) or in the $(k_p\,,\ k_d)$-plane using Eqs. (33) and (34). Hence, the 3-D global stability region can be easily obtained for the changing values of k_d in the $(k_p\,,\ k_i)$-plane or for the changing values of k_i in the $(k_p\,,\ k_d)$-plane.*

Remark 5.2. *For the neutral and retarded time-delay systems, the CRB in the $(k_i\,,\ k_d)$-plane for any k_p cannot be found directly since the gains k_i and k_d are linearly dependent on each other, which is shown in Corollary 5.1. However, to obtain the global stability region for this case, a key idea of the 2 methods in the literature, namely the singular frequencies of the parameter space approach [17] or the graphical relations of the stability boundary locus method [18], can be combined with the D-decomposition method. Since the D-decomposition method is mainly a graphical approach, the second method is selected here. With this combination, the 3-D global stability region can be now constructed by a set of 2-D convex stability regions, which are obtained for various values of k_p in the $(k_i\,,\ k_d)$-plane. For this construction, first of all, the stability intervals of the values of PID controller parameters ($k_p\,,\ k_i\,,$ and k_d) are determined. The intervals are found by the intersection of the RRB with the CRB in the $(k_p\,,\ k_i)$-plane for any value of k_d and the intersection of the IRB with the CRB in the $(k_p\,,\ k_d)$-plane for any value of k_i. Next, considering the stability intervals, a pair of CRBs for any 2 values of k_d in the $(k_p\,,\ k_i)$-plane and a couple of CRBs for any 2 values of k_i in the $(k_p\,,\ k_d)$-plane are drawn. For any k_p value, the $(k_i\,,\ k_d)$ points are determined and the stability boundary lines belonging to the 2-D convex stability region for the $(k_i\,,\ k_d)$-plane using these points are calculated. Finally, assembling these*

lines with the RRB and IRB lines, the 2-D stability region in the (k_i, k_d)-plane for the k_p selected is plotted. Changing k_p in its stability interval gives all of the 2-D stability regions, which generate the 3-D global stability region in the (k_p, k_i, k_d)-space.

5.1. Example

The second-order RTDS considered in [30] has the following state-space representation:

$$A = \begin{bmatrix} 0 & 0 \\ 0 & 1 \end{bmatrix},\ A_1 = \begin{bmatrix} -1 & -1 \\ 0 & -0.9 \end{bmatrix},\ B = \begin{bmatrix} 0 \\ 1 \end{bmatrix},\ C = \begin{bmatrix} 0 & 1 \end{bmatrix},\ \tau = 0.8. \tag{39}$$

The transfer function of the RTDS is given by:

$$G(s) = \frac{s + e^{-0.8s}}{(s^2 - s) + (1.9s - 1)e^{-0.8s} + 0.9e^{-1.6s}}. \tag{40}$$

The closed-loop system with PID controller has the following TCE:

$$P(s) = \left((k_d + 1)s^3 + (k_p - 1)s^2 + k_i s\right) + \left((k_d + 1.9)s^2 + (k_p - 1)s + k_i\right)e^{-0.8s} + 0.9se^{-1.6s}. \tag{41}$$

From Eqs. (12) and (27), the RRB and IRB are obtained as:

$$(RRB) : k_i = 0, \tag{42}$$

$$(IRB) : k_d + 1 = 0 \Rightarrow k_d = -1. \tag{43}$$

In order to get the CRB curve in the (k_p, k_i)-plane in terms of k_d, it follows from Eqs. (31) and (32) that:

$$k_p = \frac{-\omega^2 + (0.9\omega^2 + 0.9)\cos(\omega\tau) + 2\omega\sin(\omega\tau) - 0.9\omega\sin(2\omega\tau) - 1}{-\omega^2 + 2\omega\sin(\omega\tau) - 1}, \tag{44}$$

$$k_i = \frac{\left(-\omega^4 - 1.9\omega^2 + (2.9\omega^3 + 0.9)\sin(\omega\tau) + 0.9\omega^2\cos(2\omega\tau)\right) + k_d\left(-\omega^4 + 2\omega^3\sin(\omega\tau) - \omega^2\right)}{-\omega^2 + 2\omega\sin(\omega\tau) - 1}. \tag{45}$$

Selecting a k_d value ($k_d > -1$), such as $k_d = 1$, the stability boundaries and the 2-D stability region in the (k_p, k_i)-plane are shown in Figure 6a. By varying k_d and calculating the stability boundaries, many 2-D stability regions are attained for each k_d. The 3-D global stability region can then be depicted as shown in Figure 6b. As seen, the lower boundaries of the global stability region are $k_i = 0$ (RRB) in the k_i-axis and $k_d = -1$ (IRB) in the k_d-axis. In the k_p-axis, this boundary changes between 0.1 and 1.9. However, the global stability region has no upper boundaries in the 3 axes. Therefore, these axes are limited to the upper values $k_p = 4$, $k_i = 200$, and $k_d = 4$ for a good view. If the range of $k_p \in (0.1, 1.9)$ is disregarded, the global stability region can be characterized as a cube.

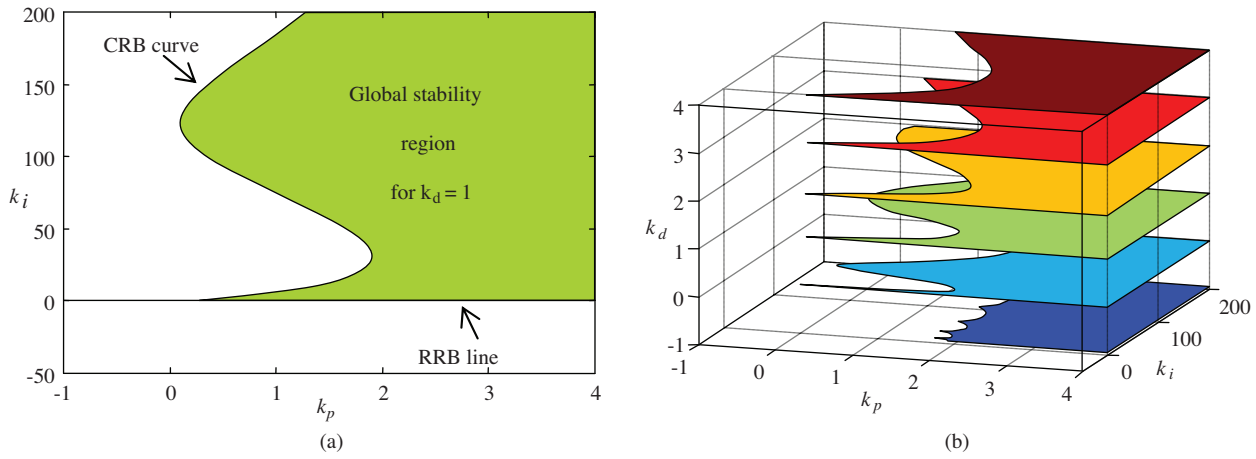

Figure 6. a) The 2-D stability region in the $(k_p,\ k_i)$-plane for $k_d = 1$ and b) the global stability region obtained by the gridding of k_d.

It is possible to use the $(k_p,\ k_d)$-plane instead of the $(k_p,\ k_i)$-plane to obtain the global stability region. From Eqs. (33) and (34), it has been calculated that k_p is the same as in Eq. (44), and k_d is found to be:

$$k_d = \frac{\left(-\omega^4 - 1.9\omega^2 + (2.9\omega^3 + 0.9)\sin(\omega\tau) + 0.9\omega^2\cos(2\omega\tau)\right) + k_i\left(\omega^2 - 2\omega\sin(\omega\tau) + 1\right)}{\omega^4 - 2\omega^3\sin(\omega\tau) + \omega^2}. \tag{46}$$

Choosing a k_i value ($k_i > 0$), such as $k_i = 1$, the 2-D stability region in the $(k_p,\ k_d)$-plane and the 3-D global stability region for the changing values of k_i are shown in Figures 7a and 7b.

The 3-D global stability region can be also obtained in the $(k_i,\ k_d)$-plane for the changing values of k_p. For this case, the global stability region consists of the 2-D convex stability regions utilizing the stability regions in the $(k_p,\ k_i)$-plane and the $(k_p,\ k_d)$-plane, as mentioned in Remark 5.2. Recall that the admissible stability ranges of the controller parameters were determined above as $k_p \in (0.1,\ \infty)$, $k_i \in (0,\ \infty)$, and $k_d \in (-1,\ \infty)$. To obtain the convex set for the values of k_p, the CRB curves in the $(k_p,\ k_i)$-plane for any 2 k_d values chosen from the range, for example $k_d = 2$ and $k_d = 3$, and in the $(k_p,\ k_d)$-plane for any 2 k_i values in the range obtained, for example $k_i = 50$ and $k_i = 60$, are shown in Figures 8a and 8b. The aim is to obtain the $(k_i,\ k_d)$ points for any k_p value in these Figures and then to constitute the equations for the $k_i - k_d$ lines across from these points. The set of these equations forms a convex stability region in the $(k_i,\ k_d)$-plane for this value of k_p. For example, let us consider the value $k_p = 1$. There are many $(k_i,\ k_d)$ points corresponding to $k_p = 1$. For better visibility, only 3 pairs are given in Figure 8a. These points and their equations for the $k_i - k_d$ lines across from these points are given as follows:

$$\text{for } (k_i, k_d) = (13.655, 3) \text{ and } (k_i, k_d) = (9.799, 2) \rightarrow k_d = 0.2593k_i - 0.5412, \tag{47}$$

$$\text{for } (k_i, k_d) = (144.091, 3) \text{ and } (k_i, k_d) = (109.394, 2) \rightarrow k_d = 0.0288k_i - 1.1528, \tag{48}$$

$$\text{for } (k_i, k_d) = (376.69, 3) \text{ and } (k_i, k_d) = (280.315, 2) \rightarrow k_d = 0.0104k_i - 0.9086, \tag{49}$$

$$\text{for } (k_i, k_d) = (768.01, 3) \text{ and } (k_i, k_d) = (579.1, 2) \rightarrow k_d = 0.0053k_i - 1.0655, \tag{50}$$

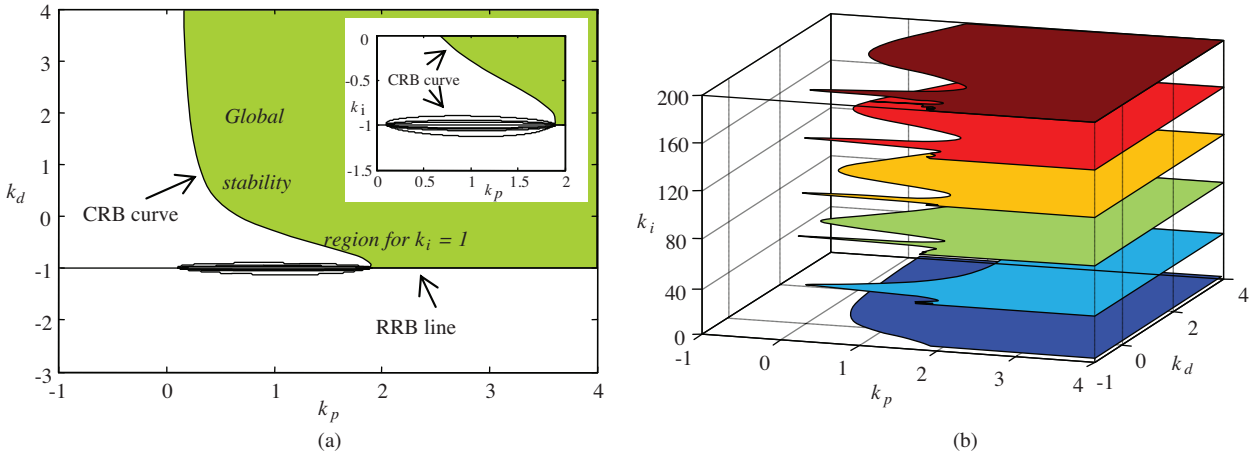

Figure 7. a) The stability region in the (k_p, k_d)-plane for $k_i = 1$ and b) the global stability region obtained by the gridding of k_i.

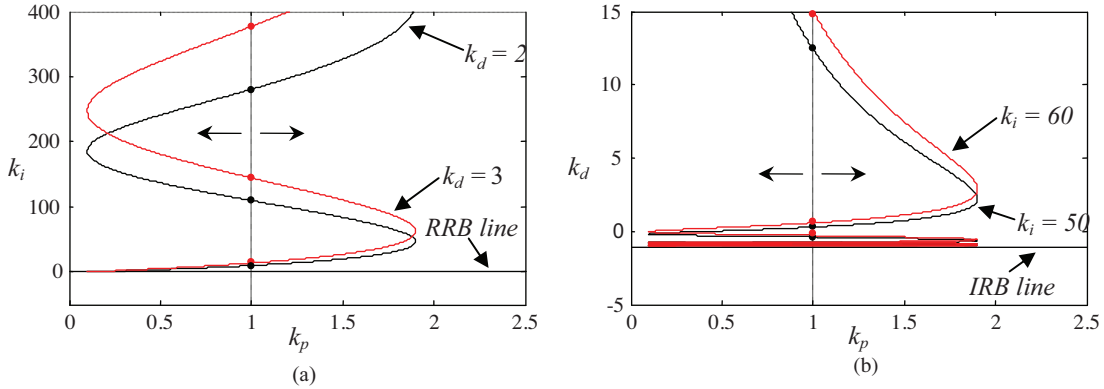

Figure 8. The points used to obtain the convex stability region in the (k_i, k_d)-plane for $k_p = 1$: a) the points in the (k_p, k_i)-plane and b) the points in the (k_p, k_d)-plane.

$$\text{for } (k_i, k_d) = (1233.22, 3) \text{ and } (k_i, k_d) = (920.94, 2) \rightarrow k_d = 0.0032k_i - 0.9491, \tag{51}$$

$$\text{for } (k_i, k_d) = (1885.4, 3) \text{ and } (k_i, k_d) = (1418.91, 2) \rightarrow k_d = 0.0021k_i - 1.0417, \tag{52}$$

$$\text{for } (k_i, k_d) = (2583.22, 3) \text{ and } (k_i, k_d) = (1931.67, 2) \rightarrow k_d = 0.0015k_i - 0.9647. \tag{53}$$

There are also a great number of points higher than the point in Eq. (53), but they can be neglected since the equations of these points come close to that of Eq. (53). Note that these equations for the $k_i - k_d$ lines can be identically obtained by the (k_p, k_d)-plane in Figure 8b.

The lines corresponding to the points in Eqs. (47) through (53), and also the RRB and IRB lines, decompose the entire plane to many areas. By testing these areas using the arbitrary check points, the multiple 2-D convex stability regions in the (k_i, k_d)-plane for $k_p = 1$ are constituted as shown in Figure 9. Repeating the procedure for the changing values of k_p, the global stability region can be sketched as a 3-D plot, shown in Figure 10. As seen, the global stability region is in the form of disconnected regions for $0.1 < k_p < 1.9$ and in the form of a 1-piece cubic region for $k_p > 1.9$.

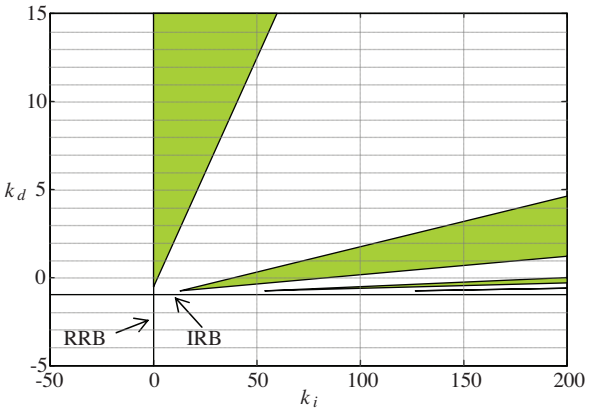

Figure 9. The 2-D convex stability region for $k_p = 1$.

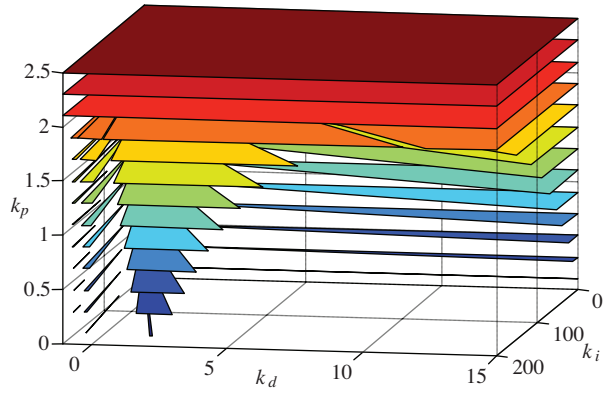

Figure 10. The global stability region obtained by the gridding of k_p in the (k_i, k_d)-plane.

6. Conclusions

The stabilization process is an important topic in the design of fixed-order controllers such as first-order, PI, and PID controllers, and it is gaining increasing attention as an effective approach to control system design for time-delay systems with or without parametric uncertainties. However, efficient stabilization algorithms are only available for the systems with time delay in the control input. In this paper, the PI and PID stabilization of a class of systems with time delay in the state, namely the neutral and retarded time-delay systems, was investigated. The principle of the method is to obtain the boundaries of the global stability region that are determined from the TCE of the closed-loop system using the D-decomposition technique. The global stability region contains the set of all of the stabilizing controller parameters. The simulation studies illustrated that the presented method provides accurate and trustworthy results.

It is known that the global stability region of a system with time delay in the control input is in the form of an enclosed area when the PI or PID controllers are used [18,31]. However, it can be concluded from Examples 4.1 and 5.1 that the global stability region for a system with state delay, i.e. a neutral or retarded system, using these controllers has no upper limits in the parameter axes. Therefore, the global stability regions of these systems are generally larger than those of the systems with control input delay.

The forthcoming trend of this study is to present an approach giving the set of optimal PI or PID controllers for the desired maximum overshoot, rise time, and settling time requirements. Such a set, which corresponds to the curves in the global stability region, provides the designer with an easier way to accomplish the control requirements. Furthermore, this study can be extended to stabilization using higher-order polynomial controllers [32].

References

[1] T. Vyhlídal, Analysis and Synthesis of Time Delay System Spectrum, PhD dissertation, Department of Instrumentation and Control Engineering, Czech Technical University, Prague, 2003.

[2] S.P. Bhattacharyya, A. Datta, L.H. Keel, Linear Control Theory: Structure, Robustness, and Optimization, Boca Raton, Florida, CRC Press, pp. 57-60, 2009.

[3] K. Gu, S.I. Niculescu, "Survey on recent results in the stability and control of time-delays systems", Journal of Dynamic Systems, Measurement, and Control, Vol. 125, pp. 158-165, 2003.

[4] K.J. Astrom, T. Hagglund, Advanced PID Control, Research Triangle Park, North Carolina, Instrumentation, Systems, and Automation Society, 2006.

[5] J.P. Richard, "Time-delay systems: an overview of some recent advances and open problems", Automatica, Vol 39, pp. 1667-1694, 2003.

[6] Z. Wang, J. Lam, K.J. Burnham, "Stability analysis and observer design for neutral delay systems", IEEE Transactions on Automatic Control, Vol. 47, pp. 478-483, 2002.

[7] V.B. Kolmanovskii, V.R. Nosov, Stability of Functional Differential Equations, London, Academic Press, 1986.

[8] M.N.A. Parlakçı, "Delay-dependent stability criteria for interval time-varying delay systems with nonuniform delay partitioning approach", Turkish Journal of Electrical Engineering & Computer Sciences, Vol. 19, pp. 763-773, 2011.

[9] W. Michiels, T. Vyhlídal, P. Zítek, "Control design for time-delay systems based on quasi-direct pole placement", Journal of Process Control, Vol. 20, pp. 337-343, 2010.

[10] T. Kubo, "Insensitivity of a class of LQ regulators of neutral systems", Electrical Engineering in Japan, Vol. 150, pp. 28-34, 2005.

[11] Y. Xia, M. Fu, P. Shi, Analysis and Synthesis of Dynamical Systems with Time Delays, Berlin, Springer-Verlag, 2009.

[12] J.G. Ziegler, N.B. Nichols, "Optimum settings for automatic controllers", Transactions of the ASME, Vol. 64, pp. 759-768, 1942.

[13] C. Knospe, "PID control," IEEE Control Systems Magazine, Vol. 26, pp. 30-31, 2006.

[14] K. Kim, Y.C. Kim, "The complete set of PID controllers with guaranteed gain and phase margins", Proceedings of the 44th IEEE Conference on Decision and Control, pp. 6533-6538, 2005.

[15] A. Datta, M.T. Ho, S.P. Bhattacharyya, Structure and Synthesis of PID Controllers, London, Springer-Verlag, 2000.

[16] N. Bajcinca, "Computation of stable regions in PID parameter space for time delay systems", Proceedings of the 5th IFAC Workshop on Time-Delay Systems, 2005.

[17] J. Ackermann, D. Kaesbauer, "Design of robust PID controllers", Proceedings of the European Control Conference, pp. 522-527, 2001.

[18] N. Tan, "Computation of stabilizing PI and PID controllers for processes with time delay", ISA Transactions, Vol. 44, pp. 213-223, 2005.

[19] Y.C. Cheng, C. Hwang, "Stabilization of unstable first-order time-delay systems using fractional-order PD controllers", Journal of the Chinese Institute of Engineers, Vol. 29, pp. 241-249, 2006.

[20] S.E. Hamamci, "An algorithm for stabilization of fractional-order time delay systems using fractional-order PID controllers", IEEE Transactions on Automatic Control, Vol. 52, pp. 1964-1969, 2007.

[21] Y.I. Neimark, "D-decomposition of the space of quasi-polynomials (on the stability of linearized distributive systems)", American Mathematical Society Translations, Vol. 102, pp. 95-131, 1973.

[22] C. Bonnet, J.R. Partington, "PID stabilization of SISO delay systems and robust stabilization of systems with multiple transmission delays", Proceedings of the Sixteenth International Symposium on Mathematical Theory of Networks and Systems, pp. 1-7, 2004.

[23] C. Bonnet, J.R. Partington, "Stabilization of a class of delay systems using PI methods", INRIA, Rapport de Recherche RR-5583, 2005.

[24] K.L. Cooke, "A linear mixed problem with derivative boundary conditions", unpublished seminar, Pomona College, 1970.

[25] J.K. Hale, S.M.V. Lunel, Introduction to Functional Differential Equations, New York, Springer, 1993.

[26] S.L. Cheng, C. Hwang, "On stabilization of time-delay unstable systems using PID controllers", Journal of the Chinese Institute of Chemical Engineers, Vol. 30, pp. 123-140, 1999.

[27] R.N. Tantaris, Stability, Performance and Robustness Using First Order Controllers, PhD dissertation, Vanderbilt University, Nashville, 2004.

[28] E.N. Gryazina, B.T. Polyak, A.A. Tremba, "D-decomposition technique state-of-the-art", Automation and Remote Control, Vol. 69, pp. 1991-2026, 2008.

[29] G.D. Hu, M. Liu, "Stability criteria of linear neutral systems with multiple delays", IEEE Transactions on Automatic Control, Vol. 52, pp. 720-724, 2007.

[30] E. Fridman, U. Shaked, "An improved stabilization method for linear time-delay systems," IEEE Transactions on Automatic Control, Vol. 47, pp. 1931-1937, 2002.

[31] N. Tan, D.P. Atherton, "Design of stabilizing PI and PID controllers", International Journal of Systems Science, Vol. 37, pp. 543-554, 2006.

[32] S.E. Hamamci, "A robust polynomial-based control for stable processes with time delay", Electrical Engineering, Vol. 87, pp. 163-172, 2005.